IEEE Access
Multidisciplinary | Rapid Review | Open Access Journal

Received September 21, 2018, accepted October 8, 2018, date of publication October 17, 2018, date of current version November 8, 2018.

Digital Object Identifier 10.1109/ACCESS.2018.2875971

Adaptive Backstepping Control Design for Uncertain Rigid Spacecraft With Both Input and Output Constraints

ZHONGTIAN CHEN, QIANG CHEN, XIONGXIONG HE, AND MINGXUAN SUN
Data-Driven Intelligent Systems Laboratory, College of Information Engineering, Zhejiang University of Technology, Hangzhou 310023, China

Corresponding author: Qiang Chen (sdnjchq@zjut.edu.cn)

This work was supported in part by the National Natural Science Foundation of China under Projects 61473262, 61573320, and 61403343, and in part by the Zhejiang Provincial Natural Science Foundation under Grant LY17F030018.

ABSTRACT In this paper, a barrier Lyapunov function (BLF)-based backstepping control design is proposed for uncertain rigid spacecraft with both input and output constraints. A modified BLF (MBLF) is constructed to extend the application scope of the traditional logarithmic BLF. Through using the MBLFs in each step of the backstepping design, an adaptive constrained control scheme is presented to guarantee the tracking performance and the constraint requirement of spacecraft systems, and the differentiation of the virtual control is avoided with the employment of the tracking differentiator. The uncertainty bounds are estimated by designing adaptive update laws, such that no prior knowledge is required on the bound of the lumped uncertainty including input saturation and faults. Numerical simulations demonstrate the effectiveness of the proposed scheme.

INDEX TERMS Barrier Lyapunov function, rigid spacecraft, backstepping design, input and output constraints.

I. INTRODUCTION

Spacecraft attitude tracking control is essential to rotate the craft to a required attitude, and it is the key factor for the success of the missions, such as formation flying, satellite communication, rendezvous of a space shuttle with the international space station, etc [1]. However, due to the nonlinear and highly coupled dynamics, it is a challenging work to design an attitude tracking controller with high precision and fast convergence for spacecraft systems with considering external disturbance and physical limitations. The problem of the spacecraft attitude control has been extensively investigated since the 1960s [2]. As two of the major issues encountered in practical spacecraft systems, the input saturation and actuator fault should be taken into account in the spacecraft attitude tracking control. In [3] and [4], the adaptive sliding mode control laws were presented for rigid spacecraft with the input saturation to achieve the attitude stabilization and tracking control, respectively. In [5], an inverse tangent-based tracking function in the backstepping-based control was designed to reduce the peak control torque for spacecraft attitude maneuver. In [6], an adaptive control method was proposed to deal with the input saturation in the spacecraft attitude stabilization without using any prior knowledge on the uncertainties. In [7], two actuator failure cases were considered for spacecraft systems, and the asymptotic stability was guaranteed by employing the sliding mode controllers. In [8], the thruster distribution matrix was utilized to deal with the actuator saturation and faults in the spacecraft system. In [9], the fuzzy logic systems (FLSs) were employed to approximate the actuator saturation and faults, and an adaptive control scheme was proposed to guarantee the satisfactory attitude tracking performance.

Driven by the theoretical challenges and practical requirements, the controller design with the constrained states has become an important research topic, and the widely used output-constrained techniques mainly include prescribed performance control (PPC) [10]–[18], barrier Lyapunov function (BLF) [19]–[27], funnel control [28]–[30] and so on. The BLF is a class of Lyapunov like function, and its value can reach the infinity when the state approaches to the boundary, such that the state is constrained within the boundary [19]. In [20] and [21], a constant logarithmic BLF and a time-varying logarithmic BLF were proposed for a class of single-input single-output (SISO) nonlinear systems to ensure the

constant output constraints and time-varying output constraints, respectively. In [23], a tangential barrier Lyapunov function (TBLF) was proposed and suitable for both the constraint and unconstraint situations, however, the introduction of the tangent function might increase the complexity of the controller design. In [24], a BLF based adaptive controller was developed for nonlinear pure-feedback systems with all the system states being constrained. In [25], a BLF based Nussbaum gain controller was constructed for SISO nonlinear systems with unknown control direction, such that all the signal constraints were guaranteed. As for the spacecraft attitude control, the constraint of angular velocity is usually imposed due to the work scenarios or sensor limitation [31]. In [32], a robust adaptive control scheme was developed for a flexible spacecraft by constructing a logarithmic BLF, and the uniform ultimate boundedness of the attitude tracking error was guaranteed as the time goes to infinity. In [33], a robust nonlinear controller was designed for the spacecraft stabilization with input saturation, and the constraint of velocity was guaranteed by using the logarithmic BLF. In [34], a logarithmic BLF based adaptive backstepping control scheme was presented for spacecraft rendezvous and proximity operations, such that the full-state constraint of the relative pose motion was achieved. In [35], an adaptive fault-tolerant controller combining the PPC and BLF was proposed to guarantee the transient and steady-state performance of the spacecraft attitude tracking.

In practice, the actuator cannot provide boundless torque and maintain health forever, hence, the input constraint including actuator saturation and faults are two unavoidable issues for spacecraft attitude control. Besides, the output constraint of the spacecraft is also a valuable practical problem for security reasons or limited by work scenarios even sensor limitation. However, the controller design of spacecraft systems with both input and output constraints remains a challenging work. On the one hand, the use of the output constraint could force the system output to converge within a prescribed bound, which is helpful to improve the system transient performance. When the initial system state is far away from the equilibrium state, the required control input is usually set relatively large to guarantee the fast transient response. But on the other hand, due to the effect of the input saturation and actuator fault, it is a hard work to keep the satisfactory transient response as usual. Consequently, it is difficult and challenging to guarantee the satisfactory transient response in the attitude control design with considering both input and output constraints.

Inspired by the aforementioned discussions, a barrier Lyapunov function based adaptive constrained control problem is addressed for the rigid spacecraft system with inertia uncertainty, external disturbance, input saturation and actuator fault. The main contributions of this paper include (i) A modified barrier Lyapunov function (MBLF) is constructed to extend the application scope of the traditional logarithmic barrier Lyapunov function, and it is suitable for both the constraint and unconstraint situations; (ii) Through

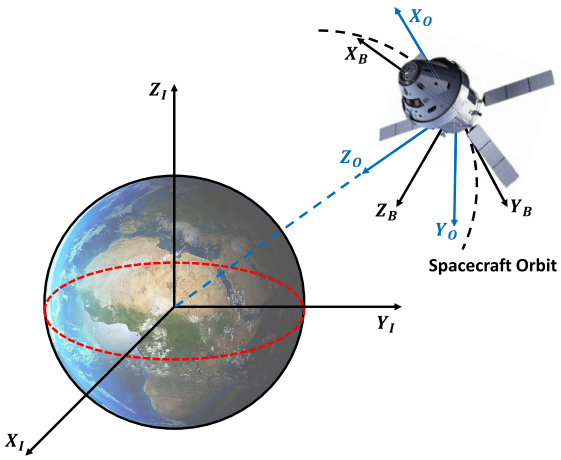

FIGURE 1. Definition of the orbit reference frame.

using the modified barrier Lyapunov functions in each step of the backstepping design, an adaptive constrained control scheme is presented to guarantee the tracking performance and the constraint requirement of spacecraft systems with input saturation and faults.

The rest of this paper is organized as follows. Section II states the formulation of the spacecraft attitude tracking problem. In Section III, a novel modified barrier Lyapunov function (MBLF) is proposed and compared with existing barrier Lyapunov functions, and an adaptive backstepping control law is presented for the spacecraft with inertia uncertainty and external disturbance. In Section IV, an adaptive fault-tolerant control scheme is proposed for the uncertain spacecraft with the input saturation. Simulation results are provided in Section V followed by the conclusion in Section VI.

II. PROBLEM FORMULATION

As shown in Fig.1, there are three main coordinate frames for the rigid spacecraft system, i.e., the inertial axis frame $\mathscr{F}(X_I, Y_I, Z_I)$, the orbit reference frame $\mathscr{F}(X_O, Y_O, Z_O)$ and the spacecraft's axis frame $\mathscr{F}(X_B, Y_B, Z_B)$. In this paper, due to the convenience of calculation without singularities, the spacecraft's attitude with respect to any reference frame is defined by the unit quaternion, which is formulated as [2]

$$q = \begin{bmatrix} n\sin(\frac{\varphi}{2}) \\ \cos(\frac{\varphi}{2}) \end{bmatrix} = \begin{bmatrix} q_v \\ q_4 \end{bmatrix} \tag{1}$$

where φ is the rotation angle, $n = [n_x, n_y, n_z]^T$ denotes the Euler axis, $q_v = [q_1, q_2, q_3]^T$ and q_4 are the vector and scalar components of the unit quaternion, respectively, and satisfy $q_v^T q_v + q_4^2 = 1$.

Then, the kinematics equations of the rigid spacecraft in terms of unit quaternion are given by

$$\begin{aligned} \dot{q}_v &= \frac{1}{2}(q_4 I_3 + q_v^{\times})\omega \\ \dot{q}_4 &= -\frac{1}{2}q_v^T \omega \end{aligned} \tag{2}$$

where I_3 is the 3×3 identity matrix, and $\omega \in R^3$ is the angular velocity of the spacecraft. The character $^\times$ denotes a skew-symmetric matrix operator for any vector $a = [a_1, a_2, a_3]^T$:

$$a^\times = \begin{bmatrix} 0 & -a_3 & a_2 \\ a_3 & 0 & -a_1 \\ -a_2 & a_1 & 0 \end{bmatrix} \tag{3}$$

which has following properties: $a^\times b = -b^\times a$ and $a^\times a = 0$, where $b = [b_1, b_2, b_3]^T$ is another vector.

The dynamics equation of spacecraft is

$$J\dot{\omega} = -\omega^\times J\omega + u + d \tag{4}$$

where $J \in R^{3\times3}$ denotes the symmetric positive definite total inertia matrix of the rigid spacecraft, $u \in R^3$ is the control torque, and $d \in R^3$ is the external disturbance with unknown upper bound.

Setting $q_d = [q_{dv}^T, q_{d4}]^T (q_{dv} := [q_{d1}, q_{d2}, q_{d3}]^T)$ as the unit quaternion of desired attitude motion, the orientation error presented by quaternion is defined as $e = [e_v^T, e_4]^T (e_v = [e_1, e_2, e_3]^T)$ in the form of

$$e_v = q_{d4}q_v - q_{dv}^\times q_v - q_4 q_{dv} \tag{5}$$

$$e_4 = q_{dv}^T q_v + q_4 q_{d4} \ . \tag{6}$$

Based on (5) and (6), the transformation from q_d to q is

$$\begin{bmatrix} q_1 \\ q_2 \\ q_3 \\ q_4 \end{bmatrix} = \begin{bmatrix} e_4 & e_3 & -e_2 & e_1 \\ -e_3 & e_4 & e_1 & e_2 \\ e_2 & -e_1 & e_4 & e_3 \\ -e_1 & -e_2 & -e_3 & e_4 \end{bmatrix} \begin{bmatrix} q_{d1} \\ q_{d2} \\ q_{d3} \\ q_{d4} \end{bmatrix}. \tag{7}$$

From (7), it is clear that when the quaternion errors reach $e_v = [0, 0, 0]^T$ and $e_4 = 1$, the accurate attitude tracking is achieved, i.e. $q = q_d$. Then, the angular velocity error is defined as

$$\omega_e = \omega - C\omega_d \tag{8}$$

where $\omega_d \in R^3$ denotes the bounded target angular velocity with the corresponding bounded derivative, $\omega_e \in R^3$ is the angular velocity error, the orthogonal matrix $C = (e_4^2 - 2e_v^T e_v)I_3 + 2e_v e_v^T - 2e_4 e_v^\times$ is the rotation matrix from the target frame to the body frame, satisfying $\|C\| = 1$, and $\dot{C} = -\omega_e^\times C$.

From (2)-(8), the attitude tracking error dynamics and kinematics are obtained by

$$\dot{e} = \begin{bmatrix} \dot{e}_v \\ \dot{e}_4 \end{bmatrix} = \frac{1}{2}\begin{bmatrix} e_4 I_3 + e_v^\times \\ -e_v^T \end{bmatrix} \omega_e \tag{9}$$

$$\begin{aligned} J\dot{\omega}_e = &-(\omega_e + C\omega_d)^\times J(\omega_e + C\omega_d) \\ &+J(\omega_e^\times C\omega_d - C\dot{\omega}_d) + u + d \end{aligned} \tag{10}$$

where $J = J_0 + \Delta J$, J_0 denotes the nonsingular known nominal value of the inertia matrix, and ΔJ is the bounded uncertainty. Substituting $J = J_0 + \Delta J$ into (10) leads to

$$\begin{aligned} \dot{\omega}_e = J_0^{-1}\big[&-\Delta J\dot{\omega}_e - (\omega_e + C\omega_d)^\times J(\omega_e + C\omega_d) \\ &+J(\omega_e^\times C\omega_d - C\dot{\omega}_d) + u + d\big] = F + J_0^{-1}u \end{aligned} \tag{11}$$

where

$$\begin{aligned} F :&= [F_1, F_2, F_3]^T \\ &= J_0^{-1}\big[-\Delta J\dot{\omega}_e - (\omega_e + C\omega_d)^\times J(\omega_e + C\omega_d) \\ &\quad +J(\omega_e^\times C\omega_d - C\dot{\omega}_d) + d\big]. \end{aligned} \tag{12}$$

Due to the boundedness of ΔJ, ω_d, $\dot{\omega}_d$, d and the fact $\|C\| = 1$, $\|\omega_e^\times\| = \|\omega_e\|$, the following inequality holds [36], [37]:

$$\begin{aligned} \|F\| \le &\left\|J_0^{-1}\right\| \|\Delta J\| \|\dot{\omega}_e\| + \left\|J_0^{-1}\right\| \|J\| \|\omega_e\|^2 \\ &+ \left\|J_0^{-1}\right\| \|J\| \|\omega_d\|^2 + \left\|J_0^{-1}\right\| \|J\| \|\omega_d\| \|\omega_e\| \\ &+ \left\|J_0^{-1}\right\| \|J\| \|\dot{\omega}_d\| + \left\|J_0^{-1}\right\| \|d\| \\ \le\ & b_1 + b_2\|\omega_e\| + b_3\|\dot{\omega}_e\| + b_4\|\omega_e\|^2 = b^T\Phi \end{aligned} \tag{13}$$

where $b = [b_1, b_2, b_3, b_4]^T$ with b_1, b_2, b_3, b_4 being unknown positive constants, and $\Phi = \left[1, \|\omega_e\|, \|\dot{\omega}_e\|, \|\omega_e\|^2\right]^T$.

From (9) and (11), the attitude tracking error dynamics and kinematics equations are formulated by

$$\begin{cases} \dot{e}_v = G\omega_e \\ \dot{\omega}_e = F + J_0^{-1}u \end{cases} \tag{14}$$

where $G = \frac{1}{2}\left(e_4 I_3 + e_v^\times\right)$. To ensure G in (14) is invertible, the condition $det(G) = e_4 \neq 0, \forall t \in [0, \infty)$ should be satisfied. It means that the initial value of e_4 is set to be nonzero, and the controller is designed to guarantee $e_4 \neq 0$ for all the time.

The control objective in this paper is to design an adaptive attitude tracking controller for rigid spacecraft (4) subject to inertia uncertainty, external disturbance, input constraint and actuator fault, such that angular velocity ω of the system is constrained, and the attitude tracking errors ω_e and e converge to a small region of the origin.

III. MBLF BASED ADAPTIVE BACKSTEPPING CONTROL

In this section, a novel modified barrier Lyapunov function is proposed for the backstepping control design of rigid spacecraft systems with inertia uncertainty and external disturbance.

A. MODIFIED BARRIER LYAPUNOV FUNCTION

The modified barrier Lyapunov function (MBLF) is presented in the form of

$$V_n(t) = \frac{1}{2}\ln\frac{k_b^2 e^{z^2}}{k_b^2 - z^2} \tag{15}$$

where $\ln(\cdot)$ is the natural logarithm, e is Euler's number, k_b is a positive constant, and the initial value of the state z is set to satisfy $|z(0)| < k_b$.

When k_b tends to the infinity, the constraint is not required and (15) becomes

$$\lim_{k_b\to\infty}\frac{1}{2}\ln\frac{k_b^2 e^{z^2}}{k_b^2 - z^2} = \frac{1}{2}z^2. \tag{16}$$

From (16), it is found that when k_b tends to the infinity, the MBLF turns into a traditional quadratic form of Lyapunov function. Therefore, compared with the traditional logarithmic BLF in [20], i.e. $V_b(t) = \frac{1}{2}\ln\frac{k_b^2}{k_b^2-z^2}$, the proposed MBLF is suitable for both the constraint and unconstraint situations, and thus extends the application scope of the traditional logarithmic barrier Lyapunov function. In order to guarantee $k_b > |z(0)|$, the value of the parameter should be selected slightly large, which may lead to unconstraint situation. However, the proposed MBLF is suitable for both the constraint and unconstraint situations, and thus the satisfactory system performance could still be guaranteed with a larger k_b.

In [23], a tangential barrier Lyapunov function (TBLF) is given by

$$V_t(t) = \frac{k_b^2}{\pi}\tan\left(\frac{\pi z^2}{k_b^2}\right), |z(0)| < k_b. \tag{17}$$

When k_b tends to the infinity, (17) has the similar property with that of MBLF, i.e.,

$$\lim_{k_b\to\infty}\frac{k_b^2}{\pi}\tan\left(\frac{\pi z^2}{k_b^2}\right) = \frac{1}{2}z^2.$$

However, differentiating (15) and (17) yields

$$\dot{V}_n = \left(1+\frac{1}{k_b^2-z^2}\right)z\dot{z} \tag{18}$$

and

$$\dot{V}_t = \frac{z\dot{z}}{\cos^2\left(\frac{\pi z^2}{2k_b^2}\right)}. \tag{19}$$

Compared with (18), the form of (19) is more complex due to the existence of cosine function in the denominator, which may hinder its application in the backstepping control design.

Lemma 1: For any positive constant k_b, the following inequality holds for the vector $z = [z_1, z_2, z_3]^T$ in the interval $\|z\| < k_b$:

$$\left(1+\frac{1}{k_b^2-z^Tz}\right)z^Tz \geq \ln\frac{k_b^2e^{z^Tz}}{k_b^2-z^Tz}. \tag{20}$$

Proof of Lemma 1: For the proof convenience, denoting $K = k_b^2$, $x_z = z^Tz$, and defining $F(x_z) = \frac{x_z}{K-x_z} - \ln\frac{K}{K-x_z}$, the derivative of $F(x_z)$ is given by

$$\dot{F}(x_z) = \frac{x_z}{(K-x_z)^2} \geq 0. \tag{21}$$

From (21), $F(x_z)$ is a monotonic increasing function, with $F(0) = 0$, and it is concluded that $F(x_z) \geq 0$ for any $x_z = z^Tz \geq 0$, i.e.,

$$\frac{z^Tz}{k_b^2-z^Tz} \geq \ln\frac{k_b^2}{k_b^2-z^Tz}. \tag{22}$$

Adding z^Tz to both sides of (22), the following inequality is easily obtained

$$\left(1+\frac{1}{k_b^2-z^Tz}\right)z^Tz \geq \ln\frac{k_b^2e^{z^Tz}}{k_b^2-z^Tz}. \tag{23}$$

This completes the proof.

B. CONTROL DESIGN

The detailed design procedures of the adaptive controller are given as follows.

Step 1: For the system (14), define two virtual states as

$$\begin{cases} z_1 = e_v \\ z_2 = \omega_e - \omega_c \end{cases} \tag{24}$$

where ω_c is the virtual control which is designed later.

Then, the following MBLF candidate is chosen as

$$V_1 = \frac{1}{2}\ln\frac{k_{b1}^2e^{z_1^Tz_1}}{k_{b1}^2-z_1^Tz_1} \tag{25}$$

where k_{b1} is the constraint on z_1, satisfying $\|z_1(0)\| < k_{b1}$.

According to (14), the time derivate of V_1 is given by

$$\dot{V}_1 = \sigma_1 z_1^T\dot{z}_1 = \sigma_1 z_1 G\omega_e \tag{26}$$

where $\sigma_1 = 1 + \frac{1}{k_{b1}^2-z_1^Tz_1}$.

Considering $\omega_e = \omega_c + z_2$, the virtual controller ω_c is designed as

$$\omega_c = -\kappa_1 G^{-1}z_1 \tag{27}$$

where $\kappa_1 > 0$ is the tunable parameter.

Substituting (27) into (26) yields

$$\dot{V}_1 = -\kappa_1\sigma_1 z_1^Tz_1 + \sigma_1 z_1^T G z_2. \tag{28}$$

Step 2: Under the condition of $\|z_2(0)\| < k_{b2}$, another BLF V_2 is given by

$$V_2 = V_1 + \frac{1}{2}\ln\frac{k_{b2}^2e^{z_2^Tz_2}}{k_{b2}^2-z_2^Tz_2} + \frac{1}{2\eta_1}\tilde{b}^T\tilde{b} \tag{29}$$

where η_1 is a positive parameter, and $\tilde{b} = b - \hat{b}$ with $\hat{b}$ being the estimation of b.

Taking the time derivative of V_2 yields

$$\dot{V}_2 = \dot{V}_1 + \sigma_2 z_2^T\dot{z}_2 - \frac{1}{\eta_1}\tilde{b}^T\dot{\hat{b}} \tag{30}$$

where $\sigma_2 = 1 + \frac{1}{k_{b2}^2-z_2^Tz_2}$.

Using (14) and (24), the time derivative of z_2 is

$$\dot{z}_2 = \dot{\omega}_e - \dot{\omega}_c = F + J_0^{-1}u - \dot{\omega}_c. \tag{31}$$

Employ the following tracking differentiator [38]

$$\begin{cases} \dot{\vartheta}_{1i} = \vartheta_{2i} \\ \dot{\vartheta}_{2i} = -r\cdot sgn(\vartheta_{1i} - \omega_{ci} + \frac{\vartheta_{2i}|\vartheta_{2i}|}{2r}), i = 1,2,3, \end{cases} \tag{32}$$

where r represents the acceleration limit of ω_c.

Then, the practical controller u in (31) is designed as

$$u=-J_0\left(\kappa_2 z_2+\frac{z_2}{\|z_2\|}\hat{b}^T\Phi+\frac{1}{2}\sigma_2 z_2+\frac{\sigma_1 e_4 e_v}{\sigma_2}-\vartheta_2\right) \quad (33)$$

and the update law of $\hat{b}$ is given by

$$\dot{\hat{b}}=\eta_1\left(\sigma_2\|z_2\|\Phi-k_1\hat{b}\right) \quad (34)$$

where $\kappa_2,\eta_1,k_1 > 0$ are design parameters, $\Phi = \left[1,\|\omega_e\|,\|\dot{\omega}_e\|,\|\omega_e\|^2\right]^T$, and $\vartheta_2=[\vartheta_{21},\vartheta_{22},\vartheta_{23}]^T$ is the output of the TD (32).

Remark 1: In most of practical applications, the derivative signal $\dot{\omega}_c$ in (31) is always difficult to obtain precisely due to the inevitable noise amplification problem. To deal with this problem, the tracking differentiator (TD) (32) is employed to approximate $\dot{\omega}_c$, which means that the TD applied in this paper can be viewed as an observer of the derivative signal $\omega_c = [\omega_{c1},\omega_{c2},\omega_{c3}]^T$. From the expressions of (14), (24) and (27), it is concluded that the boundedness of $\dot{\omega}_c$ is related to the boundedness of quaternion variables q_v, q_4 and the angular velocity ω. For practical spacecraft systems, the quaternion variables q_v and q_4 are obviously bounded because of $q_v^2+q_4^2=1$, and due to the effect of input and output constraints, the angular velocity ω is reasonable to be considered as a bounded signal. Therefore, it is feasible to employ TD (32) to estimate the bounded signal $\dot{\omega}_c$, and the rigorous proof of the TD's convergence is given in [39]. It means that there exist positive constants $\mu_{\vartheta i}, i=1,2,3$, satisfying

$$|\vartheta_{2i}-\dot{\omega}_{ci}|\le\mu_{\vartheta i}, i=1,2,3 \quad (35)$$

for $t\ge T_{td}$, where T_{td} is the settling time of the TD. It follows from (35) that

$$\|\vartheta_2-\dot{\omega}_c\|\le\mu_\vartheta \quad (36)$$

with $\dot{\omega}_c=[\dot{\omega}_{c1},\dot{\omega}_{c2},\dot{\omega}_{c3}]^T$, and μ_ϑ a positive but unknown constant.

Remark 2: The controller (33) is discontinuous when z_{2i} crosses the equilibrium point, which may lead to undesirable chattering and energy waste. This issue can be alleviated by employing the boundary layer technique [40], in which the function $\frac{z_2}{\|z_2\|}$ in (33) is replaced by

$$sig_\delta(z_2)=\left[\frac{z_{21}}{\|z_2\|+\delta},\frac{z_{22}}{\|z_2\|+\delta},\frac{z_{23}}{\|z_2\|+\delta}\right] \quad (37)$$

where $\delta > 0$ is the bounded layer parameter and its value should be chosen sufficiently small.

C. STABILITY ANALYSIS

The following theorem summarizes the stability results of the closed-loop spacecraft system.

Theorem 1: For the spacecraft system (14) with the virtual controller (27), the practical controller (33) and the update law (34), the tracking errors e_v and ω_e can converge into an arbitrarily small region of the origin when the time goes to infinity.

Proof of Theorem 1: Substituting (25) into (29) yields

$$V_2=\frac{1}{2}\ln\frac{k_{b1}^2 e^{z_1^T z_1}}{k_{b1}^2-z_1^T z_1}+\frac{1}{2}\ln\frac{k_{b2}^2 e^{z_2^T z_2}}{k_{b2}^2-z_2^T z_2}+\frac{1}{2\eta_1}\tilde{b}^T\tilde{b}. \quad (38)$$

Using (28) and (31), the time derivative of V_2 is

$$\begin{aligned}\dot{V}_2 \le& -\kappa_1\sigma_1 z_1^T z_1+\sigma_1 z_1^T G z_2\\&+\sigma_2 z_2^T\left(F+J_0^{-1}u-\dot{\omega}_c\right)-\frac{1}{\eta_1}\tilde{b}^T\dot{\hat{b}}.\end{aligned} \quad (39)$$

Substituting (33) and (34) into (39) leads to

$$\begin{aligned}\dot{V}_2 \le& -\kappa_1\sigma_1 z_1^T z_1-\kappa_2\sigma_2 z_2^T z_2+\sigma_1\left(z_1^T G z_2-e_4 z_2^T e_v\right)\\&+\sigma_2 z_2^T(\vartheta_2-\dot{\omega}_c)+\sigma_2\|z_2\|\left(\|F\|-\hat{b}^T\Phi-\tilde{b}^T\Phi\right)\\&-\frac{1}{2}\sigma_2^2\|z_2\|^2+k_1\tilde{b}^T\hat{b}.\end{aligned} \quad (40)$$

Using the fact $e_v^T e_v^\times = [0,0,0]$, $z_1^T G z_2 = e_v^T(e_4 I_3+e_v^\times)z_2 = e_4 z_2^T e_v$ is derived. According to Young's inequality and (36), the following inequality hold:

$$\sigma_2\|z_2\|\mu_\vartheta\le\frac{\sigma_2^2\|z_2\|^2}{2}+\frac{{\mu_\vartheta}^2}{2}. \quad (41)$$

Using (13) and (41), the time derivate of V_2 is further simplified as

$$\begin{aligned}\dot{V}_2 \le& -\kappa_1\left(1+\frac{1}{k_{b1}^2-z_1^T z_1}\right)z_1^T z_1\\&-\kappa_2\left(1+\frac{1}{k_{b2}^2-z_2^T z_2}\right)z_2^T z_2\\&+k_1\tilde{b}^T\hat{b}+\frac{{\mu_\vartheta}^2}{2}.\end{aligned} \quad (42)$$

According to the Lemma1, (42) is rewritten as

$$\begin{aligned}\dot{V}_2 \le& -2\kappa_1\left(\frac{1}{2}\ln\frac{k_{b1}^2 e^{z_1^T z_1}}{k_{b1}^2-z_1^T z_1}\right)\\&-2\kappa_2\left(\frac{1}{2}\ln\frac{k_{b2}^2 e^{z_1^T z_1}}{k_{b2}^2-z_2^T z_2}\right)\\&+k_1\tilde{b}^T\hat{b}+\frac{{\mu_\vartheta}^2}{2}.\end{aligned} \quad (43)$$

Using Young's inequality, the following inequality is obtained as

$$k_1\tilde{b}^T\hat{b}\le\frac{k_1}{2}b^T b-\frac{k_1}{2}\tilde{b}^T\tilde{b}. \quad (44)$$

Substituting (44) into (43) yields

$$\dot{V}_2\le-\lambda_1 V_2+\mu_1 \quad (45)$$

where $\lambda_1 = \min\{2\kappa_1,2\kappa_2\}$ with $\eta_1 = 2\kappa_1/k_1$, and $\mu_1=\frac{k_1}{2}b^T b+\frac{{\mu_\vartheta}^2}{2}$.

From (45), it is clear that the uniformly ultimate boundedness of the system tracking errors are guaranteed, and the V_2 converges to the region $V_2\le\frac{\mu_1}{\lambda_1}$, i.e.,

$$\frac{1}{2}\ln\frac{k_{b1}^2 e^{z_1^T z_1}}{k_{b1}^2-z_1^T z_1}+\frac{1}{2}\ln\frac{k_{b2}^2 e^{z_1^T z_1}}{k_{b2}^2-z_2^T z_2}+\frac{1}{2\eta_1}\tilde{b}^T\tilde{b}\le\frac{\mu_1}{\lambda_1}. \quad (46)$$

By solving (46), the region of quaternion tracking error is obtained as $\|e_v\| \leq \Delta_{z11}$, where Δ_{z11} is

$$\Delta_{z11} = \min\left\{k_{b1}\sqrt{1-\mathrm{e}^{\frac{-2\mu_1}{\lambda_1}}}, \sqrt{\frac{2\mu_1}{\lambda_1}}\right\}, \tag{47}$$

and the region of z_2 is

$$\|z_2\| \leq \Delta_{z21} = \min\left\{k_{b2}\sqrt{1-\mathrm{e}^{\frac{-2\mu_1}{\lambda_1}}}, \sqrt{\frac{2\mu_1}{\lambda_1}}\right\}. \tag{48}$$

From (47) and the property of BLF, the $e_v^T e_v$ is bounded by k_{b1} for all the time. Therefore, with the proper selection of $k_{b1} < 1$, $e_4 \neq 0$ can be easily obtained from the constraint $e_v^T e_v + e_4^2 = 1$. Hence, the boundedness of the matrix G is valid. According to the definition (27), the virtual control ω_c is also bounded, and there exists a positive constant Δ_{ω_c} satisfying $\|\omega_c\| \leq \Delta_{\omega_{c1}}$. Therefore, considering that $\omega_e = \omega_c + z_2$, the angular velocity errors converge to the region $\|\omega_e\| \leq \Delta_{\omega_{e1}} = \Delta_{z12} + \Delta_{\omega_{c1}}$. Based on the property of BLF, it is a fact that the z_1 and z_2 are constrained by k_{b1} and k_{b2}, respectively. Then, from the definition of $\omega_e = \omega_c + z_2$, $\omega = \omega_e + C\omega_d$ and the fact $\|C\| = 1$, it is concluded that the angular velocity ω of the system (4) is always constrained. This completes the proof.

Remark 3: As shown in (47), the tracking error z_1 will converge into a small region $\|z_1\| \leq \min\left\{k_{b1}\sqrt{1-\mathrm{e}^{\frac{-2\mu_1}{\lambda_1}}}, \sqrt{\frac{2\mu_1}{\lambda_1}}\right\}$ with $\lambda_1 = \min\{2\kappa_1, 2\kappa_2\}$, which means that by choosing sufficiently large parameters κ_1 and κ_2, the tracking error z_1 can converge into an arbitrarily small region when the time goes to infinity. It is equivalent to mean that for any given constant $\varepsilon > 0$, there exists a finite time t_0 such that $\|z_1\| \leq \min\left\{k_{b1}\sqrt{1-\mathrm{e}^{\frac{-2\mu_1}{\lambda_1}}}, \sqrt{\frac{2\mu_1}{\lambda_1}}\right\} + \varepsilon$ holds for $t > t_0$. Therefore, the tracking error z_1 will enter the specified bound $\min\left\{k_{b1}\sqrt{1-\mathrm{e}^{\frac{-2\mu_1}{\lambda_1}}}, \sqrt{\frac{2\mu_1}{\lambda_1}}\right\} + \varepsilon$ within a finite time.

Remark 4: The values of the parameters k_{b1}, k_{b2} should be chosen to satisfy $k_{b1} > \|z_1(0)\|, k_{b2} > \|z_2(0)\|$. The smaller k_{b1}, k_{b2} may lead to stronger constraint, and the overshoot and steady state errors could be reduced. However, too small k_{b1}, k_{b2} usually lead to the energy waste. Therefore, the tradeoff between the transient performance and energy saving must be weighed carefully when choosing the parameters.

IV. ASYMMETRIC MBLF BASED CONTROL

As a more general case of symmetric MBLF, the asymmetric MBLF is more applicable to practical systems. By adding an additional parameter to the symmetric MBLF, the upper and lower bounds of the asymmetric MBLF could be defined separately. In this section, an asymmetric MBLF is further developed for the backstepping control design of rigid spacecraft with inertia uncertainty and external disturbance.

A. CONTROL DESIGN

Step 1: For the system (24), the following asymmetric MBLF is proposed and given by

$$W_1 = \frac{1}{2}\sum_{i=1}^{3}\left[q(z_{1i})\ln\frac{k_{a1i}^2\mathrm{e}^{z_{1i}^2}}{k_{a1i}^2 - z_{1i}^2} + (1-q(z_{1i}))\ln\frac{k_{b1i}^2\mathrm{e}^{z_{1i}^2}}{k_{b1i}^2 - z_{1i}^2}\right] \tag{49}$$

where $k_{a1i} > z_{1i}(0) > -k_{b1i}, i = 1, 2, 3$ are the designed upper and lower bounds of the states, and $q(x)$ is satisfied

$$q(x) = \begin{cases} 1, & if\ x > 0 \\ 0, & if\ x \leq 0 \end{cases}. \tag{50}$$

As pointed out in [20], W_1 is piecewise smooth within each of the two intervals $z_{1i} \in (-k_{b1i}, 0]$ and $z_{1i} \in (0, k_{a1i})$. Together with the fact that $\lim_{z_1 \to 0^+} dW_1/dz_1 = \lim_{z_1 \to 0^-} dW_1/dz_1 = 0$, the conclusion is that the first derivative of W_1 is continuous.

Taking the time derivative of W_1 along (14) yields

$$\begin{aligned}\dot{W}_1 &= \sum_{i=1}^{3}\left(1 + \frac{q(z_{1i})}{k_{a1i}^2 - z_{1i}^2} + \frac{1-q(z_{1i})}{k_{b1i}^2 - z_{1i}^2}\right) z_{1i}\dot{z}_{1i} \\ &= z_1^T\Gamma_1\dot{z}_1 = z_1^T\Gamma_1 G\omega_e\end{aligned} \tag{51}$$

where $\Gamma_1 = diag\{\Gamma_{11}, \Gamma_{12}, \Gamma_{13}\}$ with $\Gamma_{1i} = 1 + \frac{q(z_{1i})}{k_{a1i}^2 - z_{1i}^2} + \frac{1-q(z_{1i})}{k_{b1i}^2 - z_{1i}^2}, i = 1, 2, 3$.

The virtual controller ω_e is designed as

$$\omega_c = -\kappa_1 G^{-1} z_1 \tag{52}$$

where $\kappa_1 > 0$ is a design parameter.

Substituting (52) into (51) leads to

$$\dot{W}_1 = -\kappa_1 z_1^T\Gamma_1 z_1 + z_1^T\Gamma_1 G z_2. \tag{53}$$

Step 2: Under the condition of $k_{a2i} > z_{2i}(0) > -k_{b2i}$, $i = 1, 2, 3$, another asymmetric MBLF is chosen as

$$\begin{aligned}W_2 = W_1 + \frac{1}{2}\sum_{i=1}^{3}\Bigg[&q(z_{2i})\ln\frac{k_{a2i}^2\mathrm{e}^{z_{2i}^2}}{k_{a2i}^2 - z_{2i}^2} \\ &+ (1-q(z_{2i}))\ln\frac{k_{b2i}^2\mathrm{e}^{z_{2i}^2}}{k_{b2i}^2 - z_{2i}^2}\Bigg] + \frac{1}{2\eta_1}\tilde{b}^T\tilde{b}\end{aligned} \tag{54}$$

where η_1 is a positive parameter, and $\tilde{b} = b - \hat{b}$.

The time derivative of W_2 is

$$\dot{W}_2 \leq \dot{W}_1 + z_2^T\Gamma_2\left(F + J_0^{-1}u - \dot{\omega}_c\right) - \frac{1}{\eta_1}\tilde{b}^T\dot{\hat{b}} \tag{55}$$

where $\Gamma_2 = diag\{\Gamma_{21}, \Gamma_{22}, \Gamma_{23}\}$ with $\Gamma_{2i} = 1 + \frac{q(z_{2i})}{k_{a2i}^2 - z_{2i}^2} + \frac{1-q(z_{2i})}{k_{b2i}^2 - z_{2i}^2}, i = 1, 2, 3$.

The practical controller u in (55) and update law of $\hat{b}$ are designed as

$$u = -J_0\left(\kappa_2 z_2 + \frac{\Gamma_2^{-1} z_2}{\|z_2\|}\|\Gamma_2\|\hat{b}^T\Phi + \frac{\|\Gamma_2\|^2\Gamma_2^{-1}}{2}z_2 + \Gamma_2^{-1}\Gamma_1 e_4 e_v - \vartheta_2\right) \tag{56}$$

$$\dot{\hat{b}} = \eta_1\left(\|\Gamma_2\|\|z_2\|\Phi - k_1\hat{b}\right) \tag{57}$$

where $\kappa_2, \eta_1, k_1 > 0$ are positive parameters, $\Phi = \left[1, \|\omega_e\|, \|\dot{\omega}_e\|, \|\omega_e\|^2\right]^T$, and $\vartheta_2 = [\vartheta_{21}, \vartheta_{22}, \vartheta_{23}]^T$ is the output of the TD (32).

B. STABILITY ANALYSIS

Theorem 2: For the spacecraft system (14) with the virtual controller (52), the practical controller (56) and the update law (57), the tracking errors e_v and ω_e can converge into an arbitrarily small region of the origin when the time goes to infinity.

Substituting (53) into (55) yields

$$\dot{W}_2 \le -\kappa_1 z_1^T\Gamma_1 z_1 + z_1^T\Gamma_1 G z_2 + z_2^T\Gamma_2\left(F + J_0^{-1}u - \dot{\omega}_c\right) - \frac{1}{\eta_1}\tilde{b}^T\dot{\hat{b}} \tag{58}$$

Using the control law (56) and update law (57), the time derivative of W_2 is

$$\dot{W}_2 \le -\kappa_1 z_1^T\Gamma_1 z_1 - \kappa_2 z_2^T\Gamma_2 z_2 + z_1^T\Gamma_1 G z_2 - e_4 z_2^T\Gamma_1 e_v + z_2^T\Gamma_2(\vartheta_2 - \dot{\omega}_c) + \|\Gamma_2\|\|z_2\|\left(\|F\| - \hat{b}^T\Phi - \tilde{b}^T\Phi\right) - \frac{1}{2}\|z_2\|^2\|\Gamma_2\|^2 + k_1\tilde{b}^T\hat{b}. \tag{59}$$

According to Young's inequality, the following inequality holds:

$$\|z_2\|\|\Gamma_2\|\mu_\vartheta \le \frac{\|\Gamma_2\|^2\|z_2\|^2}{2} + \frac{{\mu_\vartheta}^2}{2}. \tag{60}$$

From (13), (44) and (60) and using the fact $z_1^T G z_2 = e_4 z_2^T e_v$, it is obtained that

$$\dot{W}_2 \le -\kappa_1\sum_{i=1}^{3}\Gamma_{1i}z_{1i}^2 - \kappa_2\sum_{i=1}^{3}\Gamma_{2i}z_{2i}^2 - \frac{k_1}{2}\tilde{b}^T\tilde{b} + \frac{k_1}{2}b^Tb + \frac{{\mu_\vartheta}^2}{2}. \tag{61}$$

If $z_{1i} > 0$, $q(z_{1i}) = 1$, then $\Gamma_{1i} = 1 + \frac{1}{k_{a1i}^2 - z_{1i}^2}$. According to Lemma 1, it has $\left(1 + \frac{1}{k_{a1i}^2 - z_{1i}^2}\right)z_{1i}^2 \ge \ln\frac{k_{a1i}^2 e^{z_{1i}^2}}{k_{a1i}^2 - z_{1i}^2}$, and if $z_{1i} < 0$, $\left(1 + \frac{1}{k_{b1i}^2 - z_{1i}^2}\right)z_{1i}^2 \ge \ln\frac{k_{b1i}^2 e^{z_{1i}^2}}{k_{b1i}^2 - z_{1i}^2}$ holds. Consequently, the following inequalities hold with a similar deduction for z_2

$$-\sum_{i=1}^{3}\Gamma_{1i}z_{1i}^2 \le -\sum_{i=1}^{3}\left[q(z_{1i})\ln\frac{k_{a1i}^2 e^{z_{1i}^2}}{k_{a1i}^2 - z_{1i}^2} + (1 - q(z_{1i}))\ln\frac{k_{b1i}^2 e^{z_{1i}^2}}{k_{b1i}^2 - z_{1i}^2}\right] \tag{62}$$

$$-\sum_{i=1}^{3}\Gamma_{2i}z_{2i}^2 \le -\sum_{i=1}^{3}\left[q(z_{2i})\ln\frac{k_{a2i}^2 e^{z_{2i}^2}}{k_{a2i}^2 - z_{2i}^2} + (1 - q(z_{2i}))\ln\frac{k_{b2i}^2 e^{z_{2i}^2}}{k_{b2i}^2 - z_{2i}^2}\right]. \tag{63}$$

With the help of (62) and (63), the time derivative of W_2 is simplified as

$$\dot{W}_2 \le -\lambda_1 W_2 + \mu_1 \tag{64}$$

where $\lambda_1 = \min\{2\kappa_1, 2\kappa_2\}$ with $\eta_1 = 2\kappa_1/k_1$, and $\mu_1 = \frac{k_1}{2}b^Tb + \frac{{\mu_\vartheta}^2}{2}$.

By solving $W_2 \le \frac{\mu_1}{\lambda_1}$, the final region of quaternion tracking errors are $e_i = z_i \le \min\left\{K_{1i}\sqrt{1 - e^{\frac{-2\mu_1}{\lambda_1}}}, \sqrt{\frac{2\mu_1}{\lambda_1}}\right\}$, $i = 1, 2, 3$, where $K_{1i} = \max\{k_{a1i}, k_{b1i}\}$. The final region of z_2 is $z_{2i} \le \min\left\{K_{2i}\sqrt{1 - e^{\frac{-2\mu_1}{\lambda_1}}}, \sqrt{\frac{2\mu_1}{\lambda_1}}\right\}$, $i = 1, 2, 3$, where $K_{2i} = \max\{k_{a2i}, k_{b2i}\}$. Considering $\omega_c = -\kappa_1 G^{-1} z_1$ and $\omega_e = \omega_c + z_2$, ω_e can converge into an arbitrarily small region of the origin when the time goes to infinity. According to [20], the signals z_{1i} and $z_{2i}, i = 1, 2, 3$ remain in the compact $(-k_{b1i}, k_{a1i})$ and $(-k_{b2i}, k_{a2i})$, respectively. Hence, all the states of the system are bounded, and the transient and steady-state performance of the output ω can be improved by tuning the asymmetric MBLF parameters. As pointed out in Remark 3, if the parameters κ_1 and κ_2 are chosen sufficiently large, $2\mu_1/\lambda_1$ leads to 0, which implies that ω_e can converge into an arbitrarily small region $\Delta_{\omega e2}$ in infinite time. It is equivalent to mean that for any given constant $\varepsilon > 0$, the tracking error ω_e will enter the specific bound $\|\omega_e\| \le \Delta_{\omega e2} + \varepsilon$ within a finite time. This completes the proof.

V. FAULT-TOLERANT CONTROL WITH INPUT SATURATION

In this section, the input constraint and actuator fault are both taken into account. By incorporating MBLF in the adaptive backstepping design, the adaptive fault-tolerant controller is developed to ensure that the tracking errors are driven into a small region of the origin in the presence of angular velocity constraint.

A. CONTROL DESIGN

Considering the input saturation and actuator fault, the equation (4) is re-expressed as

$$J\dot{\omega} = -\omega^\times J\omega + Dsat(u) + d \tag{65}$$

where $D = diag\{D_1, D_2, D_3\}$ is the actuator effectiveness, $D_i(t) = 1$ means that the ith actuator is totally health, $0 < D_i(t) \leq 1$ represents that the ith actuator has lost its effectiveness partially, and $sat(u) = [sat(u_1), sat(u_2), sat(u_3)]^T$ is the saturated control given by

$$sat(u_i) = \begin{cases} u_{mi}, & if\ u_i > u_{mi} \\ u_i, & if\ -u_{mi} \leq u_i \leq u_{mi} \\ -u_{mi}, & if\ u_i < -u_{mi} \end{cases} \tag{66}$$

where u_{mi} and $-u_{mi}$ are the maximum and minimum torque that ith axis provides, respectively.

For the convenience of the controller design, the saturation function $sat(u)$ is expressed as

$$sat(u) = \chi(u(t)) \cdot u(t) \tag{67}$$

where $\chi(u(t)) = diag\{\chi_1(u_1(t)), \chi_2(u_2(t)), \chi_3(u_3(t))\}$ and

$$\chi_i(u_i(t)) = \begin{cases} u_{mi}/u_i, & if\ u_i > u_{mi} \\ 1, & if\ -u_{mi} \leq u_i \leq u_{mi} \\ -u_{mi}/u_i, & if\ u_i < -u_{mi} \end{cases}. \tag{68}$$

The coefficient $0 < \chi_i(u_i(t)) \leq 1$ reflects the saturation degree of the ith axis of the control torque. Since $0 < D_i(t) \leq 1$ and $0 < \chi_i(u_i(t)) \leq 1$, it is reasonable to assume that there exists a constant ξ satisfying

$$0 < \xi \leq \min\{D_i(t)\chi_i(u_i(t)), i = 1, 2, 3\} \leq 1. \tag{69}$$

From (9), (65) and (67), the rigid spacecraft attitude tracking dynamics and kinematics equations with input saturation and actuator fault are obtained by

$$\begin{cases} \dot{e}_v = G\omega_e \\ \dot{\omega}_e = F + J_0^{-1} D\chi(u(t)) \cdot u(t) \end{cases} \tag{70}$$

Following the similar backstepping procedures of the former sections, the virtual controller and the practical controller based on the MBLF (15) are designed as

$$\omega_c = -\kappa_1 G^{-1} z_1, \tag{71}$$

and

$$u = -J_0 \left[\kappa_2 z_2 + \frac{z_2}{\|z_2\|} \hat{\gamma} \left(\frac{\sigma_1}{\sigma_2} |e_4| \|e_v\| + u_m \right) \right], \tag{72}$$

where κ_1, κ_2 are tunable parameters, $\hat{\gamma}$ is the estimation of ξ^{-1}, $\sigma_1 = 1 + \frac{1}{k_{b1}^2 - z_1^T z_1}$, $\sigma_2 = 1 + \frac{1}{k_{b2}^2 - z_2^T z_2}$, the function u_m is

$$u_m = \hat{b}^T \Phi + \|\vartheta_2\| + \frac{1}{2}\sigma_2 \|z_2\|, \tag{73}$$

where $\hat{b}$ is the estimation of b, $\Phi = \left[1, \|\omega_e\|, \|\dot{\omega}_e\|, \|\omega_e\|^2\right]^T$, and $\vartheta_2 = [\vartheta_{21}, \vartheta_{22}, \vartheta_{23}]^T$ is the output of the TD (32). The update laws of $\hat{b}$ and $\hat{\gamma}$ are

$$\dot{\hat{b}} = \eta_1 \left(\sigma_2 \|z_2\| \Phi - k_1 \hat{b} \right), \tag{74}$$

$$\dot{\hat{\gamma}} = \eta_2 \left[\hat{\gamma}^3 \left(\sigma_1 |e_4| \|e_v\| \|z_2\| + \sigma_2 \|z_2\| u_m \right) + k_2 \hat{\gamma} \right], \tag{75}$$

where η_1, η_2, k_1, k_2 are positive parameters.

B. STABILITY ANALYSIS

Theorem 3: For the spacecraft system (70) subject to input saturation and actuator fault, with the virtual controller (71), the practical controller (72), and the update laws (74) and (75), the tracking errors e_v and ω_e can converge into an arbitrarily small region of the origin when the time goes to infinity.

Proof of Theorem 3: Define a positive MBLF as

$$V_3 = \frac{1}{2} \ln \frac{k_{b1}^2 e^{z_1^T z_1}}{k_{b1}^2 - z_1^T z_1} + \frac{1}{2} \ln \frac{k_{b2}^2 e^{z_2^T z_2}}{k_{b2}^2 - z_2^T z_2} + \frac{1}{2\eta_1} \tilde{b}^T \tilde{b} + \frac{1}{2\eta_2} \tilde{\gamma}^2 \tag{76}$$

where $z_1 = e_v$, $z_2 = \omega_e - \omega_c$, $\tilde{b} = b - \hat{b}$, and $\tilde{\gamma} = \xi - \hat{\gamma}^{-1}$.

Using (70) and (71), the time derivative of V_3 is

$$\begin{aligned} \dot{V}_3 \leq & -\kappa_1 \sigma_1 z_1^T z_1 + \sigma_1 z_1^T G z_2 - \frac{1}{\eta_1} \tilde{b}^T \dot{\hat{b}} + \frac{1}{\eta_2} \tilde{\gamma} \hat{\gamma}^{-2} \dot{\hat{\gamma}} \\ & + \sigma_2 z_2^T \left(F + J_0^{-1} D sat(u) - \dot{\omega}_c \right). \end{aligned} \tag{77}$$

Substituting (72)-(75) into (77) and using the property (69) lead to

$$\begin{aligned} \dot{V}_3 \leq & -\kappa_1 \sigma_1 z_1^T z_1 - \kappa_2 \sigma_2 \xi z_2^T z_2 \\ & + \sigma_1 \left[{z_1}^T G z_2 - (\xi - \tilde{\gamma}) \hat{\gamma} |e_4| \|e_v\| \|z_2\| \right] \\ & + \sigma_2 \|z_2\| \left[\|F\| - (\xi - \tilde{\gamma}) \hat{\gamma} \hat{b}^T \Phi - \tilde{b}^T \Phi \right] \\ & + \sigma_2 \|z_2\| \left[\|\dot{\omega}_c\| - (\xi - \tilde{\gamma}) \hat{\gamma} \|\vartheta_2\| \right] \\ & - \frac{1}{2} \sigma_2^2 \|z_2\|^2 (\xi - \tilde{\gamma}) \hat{\gamma} + k_1 \tilde{b}^T \hat{b} + k_2 \tilde{\gamma} \hat{\gamma}^{-1}. \end{aligned} \tag{78}$$

From (36), (41) and using the fact $z_1^T G z_2 = e_4 z_2^T e_v$, $\xi - \tilde{\gamma} = \hat{\gamma}^{-1}$, the time derivate of V_3 is further simplified as

$$\begin{aligned} \dot{V}_3 \leq & -\kappa_1 \left(1 + \frac{1}{k_{b1}^2 - z_1^T z_1} \right) z_1^T z_1 \\ & - \kappa_2 \left(1 + \frac{1}{k_{b2}^2 - z_2^T z_2} \right) \xi z_2^T z_2 \\ & + k_1 \tilde{b}^T \hat{b} + k_2 \tilde{\gamma} \hat{\gamma}^{-1} + \frac{{\mu_\vartheta}^2}{2}. \end{aligned} \tag{79}$$

According to Lemmas 1, (79) is rewritten as

$$\begin{aligned} \dot{V}_3 \leq & -2\kappa_1 \left(\frac{1}{2} \ln \frac{k_{b1}^2 e^{z_1^T z_1}}{k_{b1}^2 - z_1^T z_1} \right) \\ & - 2\kappa_2 \xi \left(\frac{1}{2} \ln \frac{k_{b2}^2 e^{z_2^T z_2}}{k_{b2}^2 - z_2^T z_2} \right) \\ & + k_1 \tilde{b}^T \hat{b} + k_2 \tilde{\gamma} \hat{\gamma}^{-1} + \frac{{\mu_\vartheta}^2}{2}. \end{aligned} \tag{80}$$

Using Young's inequality, the following inequality is obtained as

$$k_2 \tilde{\gamma} \hat{\gamma}^{-1} = k_2 \tilde{\gamma} (\xi - \tilde{\gamma}) \leq \frac{k_2}{2} \xi^2 - \frac{k_2}{2} \tilde{\gamma}^2. \tag{81}$$

Substituting (44) and (81) into (80) yields

$$\dot{V}_3 \leq -\lambda_2 V_3 + \mu_2 \tag{82}$$

where $\lambda_2 = \min\{2\kappa_1, 2\xi\kappa_2\}$ with $\eta_1 = 2\kappa_1/k_1$, $\eta_2 = 2\kappa_1/k_2$, and $\mu_2 = \frac{k_1}{2}b^T b + \frac{k_2}{2}\xi^2 + \frac{\mu_\vartheta^2}{2}$.

From (82), it is concluded that $V_3 \leq \frac{\mu_2}{\lambda_2}$ when the time goes to infinity, and the uniformly ultimate boundedness of the system tracking errors are guaranteed. Furthermore, the quaternion tracking error e_v and angular velocity error ω_e converge to the region $\|e_v\| \leq \Delta_{z_{21}} = \min\left\{k_{b1}\sqrt{1-\mathrm{e}^{\frac{-2\mu_2}{\lambda_2}}}, \sqrt{\frac{2\mu_2}{\lambda_2}}\right\}$ and $\|\omega_e\| \leq \Delta_{\omega_{e3}} = \Delta_{z_{22}} + \Delta_{\omega_{c2}}$, respectively. $\Delta_{z_{22}} = \min\left\{k_{b2}\sqrt{1-\mathrm{e}^{\frac{-2\mu_2}{\lambda_2}}}, \sqrt{\frac{2\mu_2}{\lambda_2}}\right\}$ is region of z_2 and $\Delta_{\omega_{c2}}$ is the region of ω_c. Using the property of MBLF, it is obtained that z_1 and z_2 are constrained by k_{b1} and k_{b2}. Therefore, considering the definition of ω, the constraint of the angular velocity ω in the system (65) is guaranteed. This completes the proof.

VI. NUMERICAL SIMULATIONS

In order to illustrate the effectiveness of the proposed adaptive controllers, the simulations and corresponding discussions are presented in this section. The spacecraft model is given by (14), where the initial state values are set as

$$q(0) = [-0.1, 0.5, -0.2, \sqrt{0.7}]^T,$$
$$\omega(0) = [0.01, -0.01, 0.01]^T \ rad/s.$$

The desired attitude motion is given by

$$q_d = [0, 0, 0, 1]^T,$$
$$\omega_d = 0.1[\cos(t/40), -\sin(t/50), -\cos(t/60)]^T \ rad/s.$$

The nominal inertia matrix $J_0 = diag\{45, 42, 37.5\}$, and the uncertainty ΔJ is

$$\Delta J = diag\{4, 3.5, 2\}(1 + e^{-0.1t}) - 2\Delta J_1 \ kg \cdot m^2$$

where

$$\Delta J_1 = \begin{cases} 0, & t < 5 \\ I_3, & t \geq 5 \end{cases}.$$

The external disturbance is

$$d = 0.5\|\omega\|[\sin(0.8t), \cos(0.5t), \sin(0.3t)]^T \ N \cdot m.$$

A. ATTITUDE TRACKING FOR SPACECRAFT WITH INERTIA UNCERTAINTY AND EXTERNAL DISTURBANCE

In this subsection, the attitude tracking control performance with inertia uncertainty and external disturbance is shown to illustrate the effectiveness of the proposed control scheme (27), (33)-(32) in Section III. The parameters of the controllers and update laws are set as $\kappa_1 = 0.2, \kappa_2 = 0.4$, $k_{b1} = 0.8, k_1 = 0.2, \eta_1 = 2, r = 0.5$, and the initial values of $\hat{b}$ is set as $[0.01, 0.01, 0.01, 0.01]^T$. In order to verify the effect of the MBLF parameter k_{b2} on the tracking

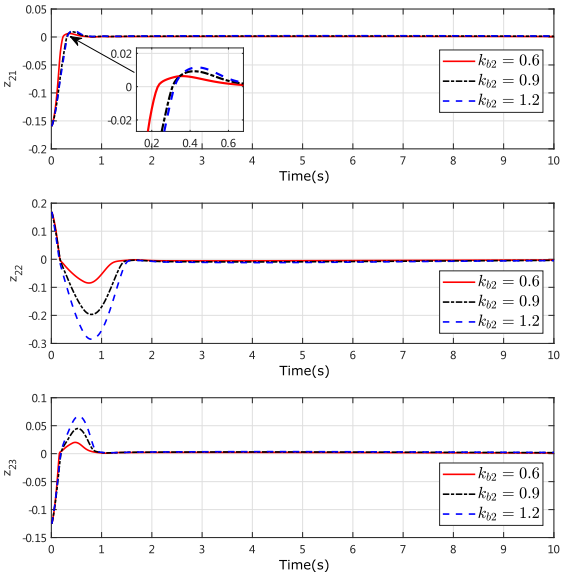

FIGURE 2. Virtual state z_2.

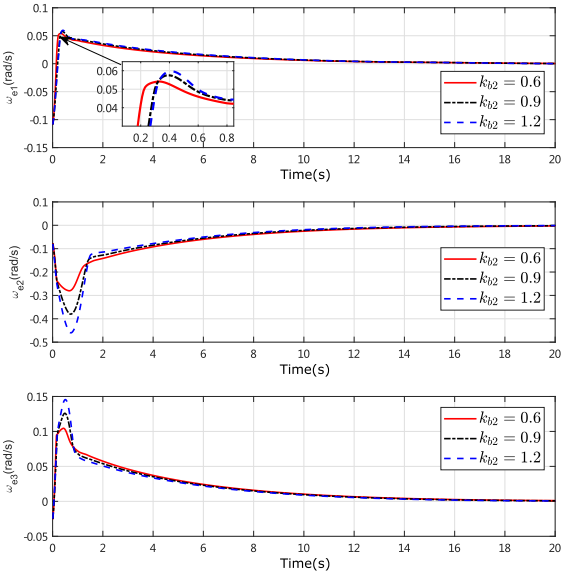

FIGURE 3. Angular velocity tracking errors ω_e.

performance, the compared simulations are conducted with different selection of k_{b2}, i.e., $k_{b2} = 0.6$, 0.9, and 1.2.

Fig.2 and Fig.3 depict virtual state z_2 and angular velocity errors ω_e of the spacecraft system, respectively. From Figs.2 and 3, it is seen that the satisfactory attitude tracking performance is achieved, and the overshoot is smaller when the parameter k_{b2} is set to be 0.6. It means that the constraint effect is better with the smaller k_{b2}. The control torque u is shown in Fig.4, which states that the undesirable chattering is eliminated in the controller by using the boundary layer technique (37). Fig.5 shows that the for $k_{b2} = 0.6$ quaternion errors $e = [e_1, e_2, e_3, e_4]^T$ converge to the small neighborhoods of zero and $e_4 \neq 0$, which is consistent with the theoretical analysis. Fig.6 depicts the performance

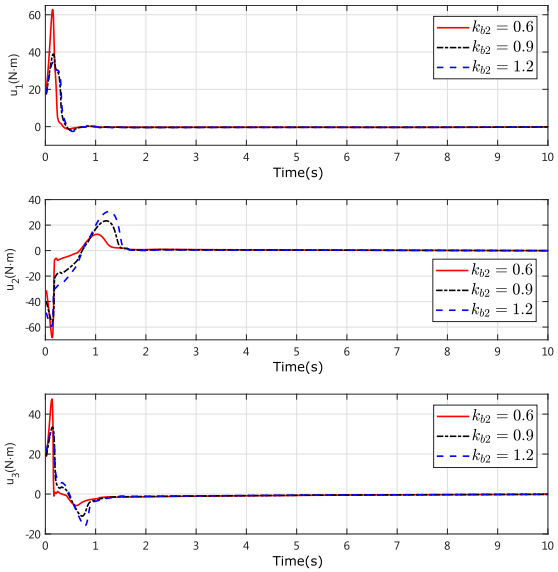

FIGURE 4. Control torque u.

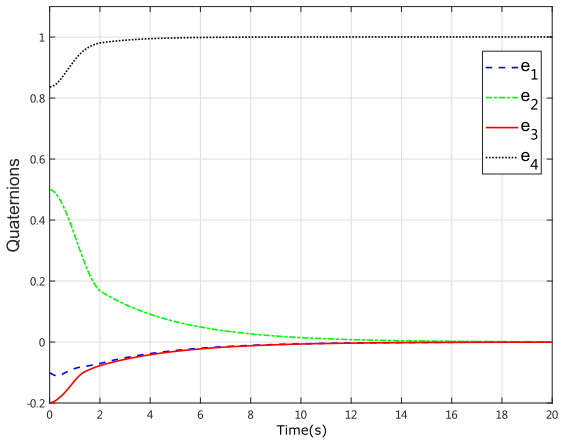

FIGURE 5. Quaternion tracking errors e with $k_{b2} = 0.6$.

of the tracking differentiator, which shows that the TD is capable of approximating $\dot{\omega}_c$ within 3 seconds. The convergence performance of the estimated parameter $\hat{b}$ is shown in Fig.7, and it is clear that the parameter $\hat{b}$ converges to the positive constant. The uncertainty estimation is depicted in Fig.8, which shows that the inequality (13) is reasonable and the update law accomplishes the scheduled purpose. From Figs.2-8, it is concluded that the proposed controller can achieve precise attitude tracking in the presence of the external disturbance and inertia uncertainty, and the smaller k_{b2} reduces the overshoot of the constrained angular velocity.

B. ATTITUDE TRACKING FOR SPACECRAFT WITH ASYMMETRIC MBLF

In this subsection, two schemes including the asymmetric MSLF (AMBLF) based control in Section IV and symmetric MBLF (SMBLF) based control in Section III are provided for the comparison.

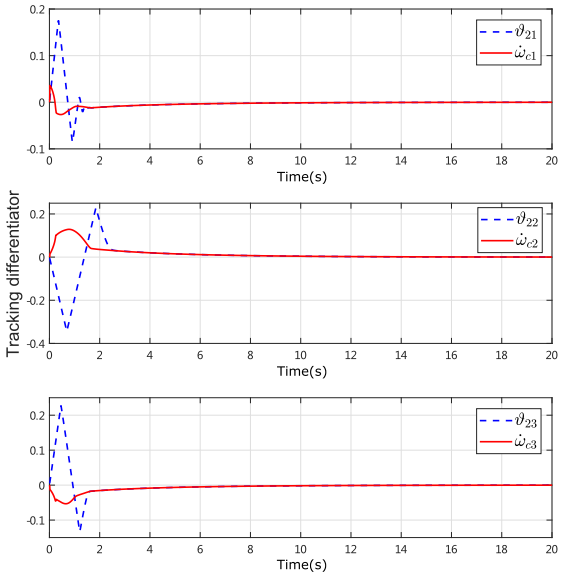

FIGURE 6. Tracking differentiator approximation with $k_{b2} = 0.6$.

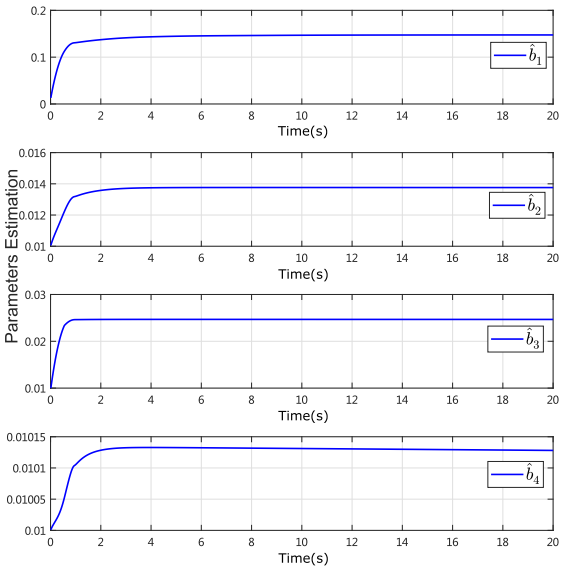

FIGURE 7. Estimated parameter $\hat{b}$ with $k_{b2} = 0.6$.

TABLE 1. Constraint parameters for z_2.

States	z_{21}	z_{23}	z_{23}
AMBLF	$k_{a21} = 0.4$	$k_{a22} = 0.6$	$k_{a23} = 0.4$
	$k_{b21} = 0.6$	$k_{b22} = 0.4$	$k_{b23} = 0.6$
SMBLF	$k_{b2} = 0.6$	$k_{b2} = 0.6$	$k_{b2} = 0.6$

Most parameters in both schemes are set the same, i.e., $\kappa_1 = 0.2, \kappa_2 = 0.4, k_1 = 0.2, \eta_1 = 2, r = 0.5$, $k_{a1i} = k_{b1i} = k_{b1} = 0.8, i = 1, 2, 3$, and the initial values of $\hat{b}$ is set as $[0.01, 0.01, 0.01, 0.01]^T$. The different constraint parameters are set and shown in Table 1.

The comparative simulation results of AMBLF and SMBLF are shown in Figs.9 and 10, which depict virtual state z_2 and angular velocity errors ω_e of the spacecraft

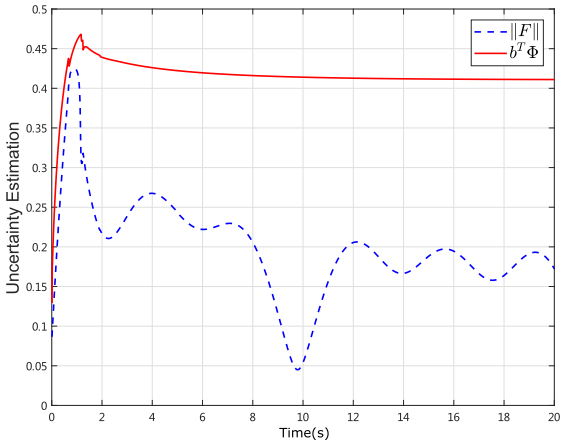

FIGURE 8. Estimated uncertainty with $k_{b2} = 0.6$.

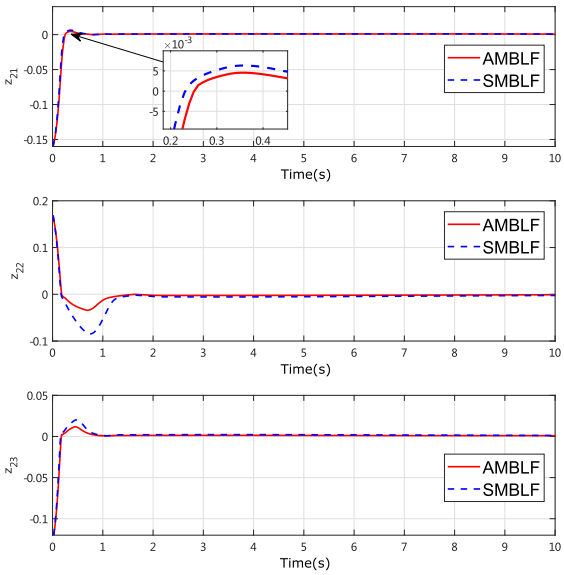

FIGURE 9. Virtual state z_2.

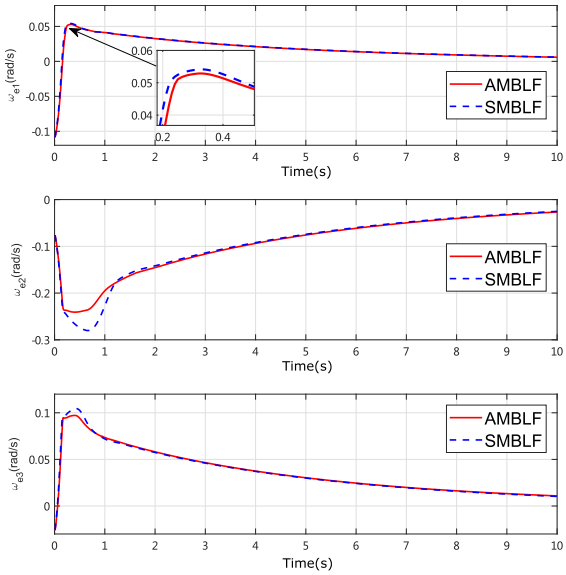

FIGURE 10. Angular velocity tracking errors ω_e.

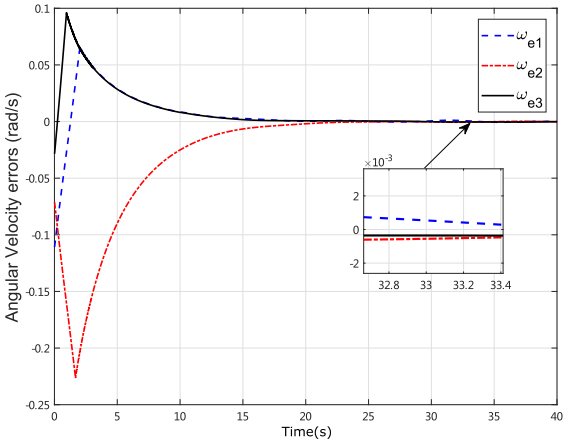

FIGURE 11. Angular velocity errors ω_e with C1.

system, respectively. From Figs.9 and 10, it is seen that compared with SMBLF method, the AMBLF has the better convergence rate and less overshoot, which means that the AMBLF based control can achieve the improved transient performance by tuning parameters.

C. ATTITUDE TRACKING FOR SPACECRAFT WITH INPUT SATURATION AND ACTUATOR FAULTS

In this subsection, the attitude tracking control performance for the spacecraft with input saturation and actuator faults is provided, and to show the good property of the proposed MBLF, the conventional logarithmic BLF [20] based control scheme is employed for the comparison.

For the notation convenience, the two control schemes are given as follows.

C1: The proposed control scheme based on the MBLF, including virtual control law (71), control law (72), update laws (74) and (75).

C2: The control scheme based on the logarithmic BLF [20].

The constraint of the input is $|u_i| \leq 5\ N \cdot m, i = 1, 2, 3$ and the actuator fault condition $D = diag\{D_1, D_2, D_3\}$ is

$$D_i(t) = \begin{cases} 1, & if\ t < 10s \\ 0.75 + 0.1\sin(0.5t + i\pi/3), & if\ t \geq 10s \end{cases}.$$

The control parameters in C1 and C2 are set the same, i.e., $\kappa_1 = 0.25, \kappa_2 = 0.4, k_1 = 0.01, k_2 = 0.15, \eta_1 = 50, \eta_2 = 1/3, r = 0.2$. The initial values of $\hat{b}$ and $\hat{\gamma}$ are set as $[0.01, 0.01, 0.01, 0.01]^T$ and 0.15, respectively. In order to express the unconstraint situation, k_{b1} and k_{b2} are set sufficiently large, i.e., $k_{b1} = 10, k_{b2} = 10$.

The comparative simulation results of C1 and C2 are shown in Figs.11-14. The attitude tracking angular velocity errors of C1 and C2 are depicted in Figs.11 and 12, and the average angular velocity errors after 20s are 3.347×10^{-4} and 0.013, respectively. As shown in Figs.11 and 12, the proposed C1 scheme can still achieve the satisfying attitude

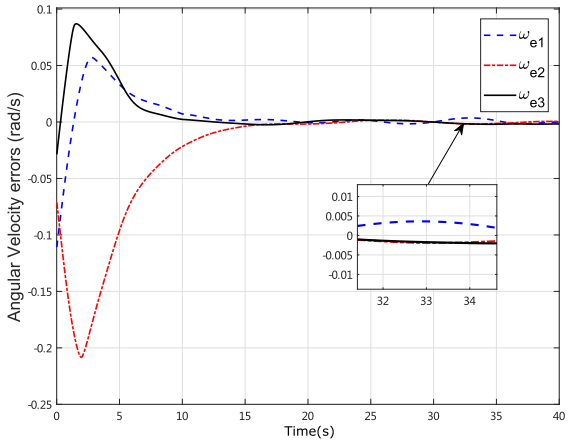

FIGURE 12. Angular velocity errors ω_e with C2.

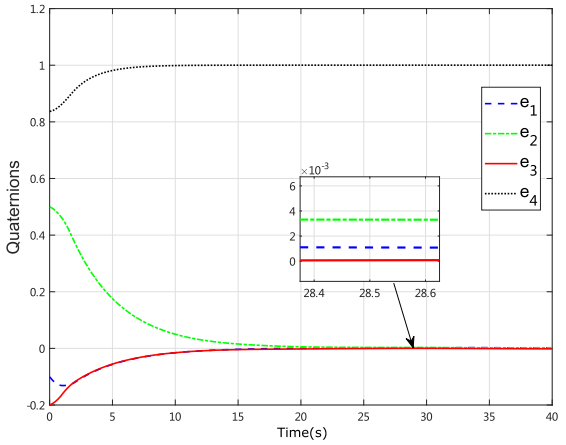

FIGURE 13. Quaternion tracking errors e with C1.

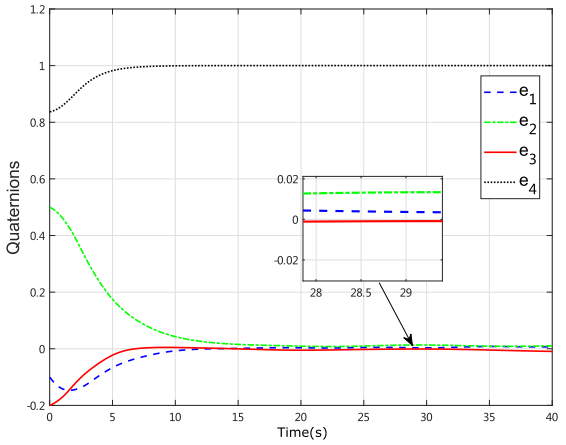

FIGURE 14. Quaternion tracking errors e with C2.

tracking performance with larger k_{b1} and k_{b2}, but the performance of C2 scheme becomes worse with the same parameters. The quaternion errors of C1 and C2 are shown in Figs.13 and 14, and the average quaternion errors after 20s are 0.013 and 0.056, respectively. Fig.13 shows that the

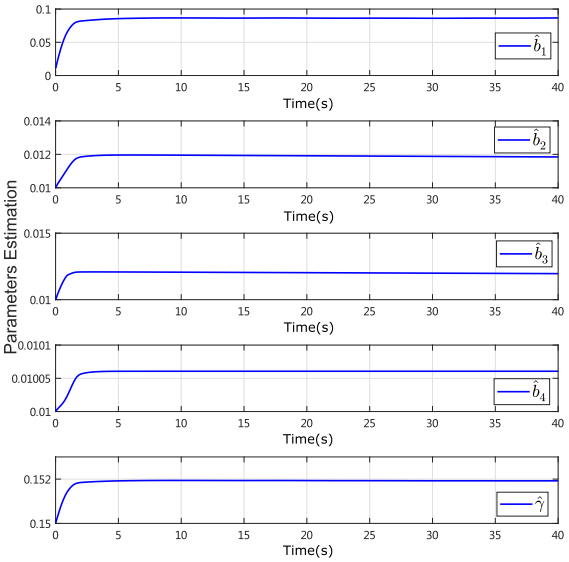

FIGURE 15. Estimated parameters $\hat{b}$ and $\hat{\gamma}$ with C1.

quaternion errors of C1 converge to the small neighborhood of zero. However, as shown in Fig.14, the static quaternion errors of C2 are larger than those of C1. The convergence performance of the estimated parameters $\hat{b}$ and $\hat{\gamma}$ of C1 is shown in Fig.15. From Figs.11-15, it is concluded that the proposed C1 scheme can achieve the precise tracking performance in the presence of the external disturbance, inertia uncertainty, actuator fault, as well as input and output constraints. Furthermore, it is verified that the novel MBLF can be effective for both constraint and unconstraint situations, which is consistent with the theoretical analysis given in Section III.

VII. CONCLUSION

The attitude tracking problem has been investigated in this paper for spacecraft systems with both input and output constraints. The application scope of the traditional logarithmic barrier Lyapunov function is extended by constructing a novel modified barrier Lyapunov function (MBLF) suitable for constraint and unconstraint situations. Then, the adaptive controller is proposed through the backstepping design with MBLF, and the derivative signal of the virtual controller is estimated by using the tracking differentiator. With the proposed control scheme, the knowledge on the bound of the lumped uncertainty is not required in prior, and simulation examples are provided to verify the effectiveness of the proposed scheme.

REFERENCES

[1] M. J. Sidi, *Spacecraft Dynamics and Control: A Practical Engineering Approach*. Cambridge, U.K.: Cambridge Univ. Press, 1997.
[2] B. P. Ickes, "A new method for performing digital control system attitude computations using quaternions," *Amer. Inst. Aeronaut. Astronaut.*, vol. 8, no. 1, pp. 13–17, Jan. 1970.
[3] J. D. Boškovic, S.-M. Li, and R. K. Mehra, "Robust adaptive variable structure control of spacecraft under control input saturation," *J. Guid., Control, Dyn.*, vol. 24, no. 1, pp. 14–22, 2001.

[4] J. D. Boskovic, S.-M. Li, and R. K. Mehra, "Robust tracking control design for spacecraft under control input saturation," *J. Guid., Control, Dyn.*, vol. 27, no. 4, pp. 627–633, Jul. 2004.
[5] I. Ali, G. Radice, and J. Kim, "Backstepping control design with actuator torque bound for spacecraft attitude maneuver," *J. Guid., Control, Dyn.*, vol. 33, no. 1, pp. 254–259, Jan. 2010.
[6] Z. Zhu, Y. Xia, and M. Fu, "Adaptive sliding mode control for attitude stabilization with actuator saturation," *IEEE Trans. Ind. Electron.*, vol. 58, no. 10, pp. 4898–4907, Oct. 2011.
[7] K. D. Kumar, "Robust attitude stabilization of spacecraft subject to actuator failures," *Acta Astronaut.*, vol. 68, no. 7, pp. 1242–1259, Apr./May 2011.
[8] W. Cai, X. Liao, and D. Y. Song, "Indirect robust adaptive fault-tolerant control for attitude tracking of spacecraft," *J. Guid., Control, Dyn.*, vol. 31, no. 5, pp. 1456–1463, Sep. 2008.
[9] B. Huo, Y. Xia, L. Yin, and M. Fu, "Fuzzy adaptive fault-tolerant output feedback attitude-tracking control of rigid spacecraft," *IEEE Trans. Syst., Man, Cybern. Syst.*, vol. 47, no. 8, pp. 1898–1908, Aug. 2017.
[10] C. P. Bechlioulis and G. A. Rovithakis, "Robust adaptive control of feedback linearizable MIMO nonlinear systems with prescribed performance," *IEEE Trans. Autom. Control*, vol. 53, no. 9, pp. 2090–2099, Oct. 2008.
[11] C. P. Bechlioulis and G. A. Rovithakis, "Adaptive control with guaranteed transient and steady state tracking error bounds for strict feedback systems," *Automatica*, vol. 45, no. 2, pp. 532–538, 2009.
[12] M. Chen, Q. Wu, C. Jiang, and B. Jiang, "Guaranteed transient performance based control with input saturation for near space vehicles," *Sci. China Inf. Sci.*, vol. 57, no. 5, pp. 1–12, 2014.
[13] Q. Chen, L. Shi, J. Na, X. Ren, and Y. Nan, "Adaptive echo state network control for a class of pure-feedback systems with input and output constraints," *Neurocomputing*, vol. 275, pp. 1370–1382, Jan. 2018.
[14] J. Na, Q. Chen, X. Ren, and Y. Guo, "Adaptive prescribed performance motion control of servo mechanisms with friction compensation," *IEEE Trans. Ind. Electron.*, vol. 61, no. 1, pp. 486–494, Jan. 2014.
[15] J. Na, Y. Huang, X. Wu, G. Gao, G. Herrmann, and J. Z. Jiang, "Active adaptive estimation and control for vehicle suspensions with prescribed performance," *IEEE Trans. Control Syst. Technol.*, vol. 26, no. 6, pp. 2063–2077, Nov. 2017, doi: 10.1109/TCST.2017.2746060.
[16] S. Wang, J. Na, and X. Ren, "RISE-based asymptotic prescribed performance tracking control of nonlinear servo mechanisms," *IEEE Trans. Syst., Man, Cybern. Syst.*, to be published, doi: 10.1109/TSMC.2017.2769683.
[17] Q. Chen, S. Xie, M. Sun, and X. He, "Adaptive non-singular fixed-time attitude stabilization of uncertain spacecraft," *IEEE Trans. Aerosp. Electron. Syst.*, to be published, doi: 10.1109/TAES.2018.2832998.
[18] C. Yang, Y. Jiang, Z. Li, W. He, and C.-Y. Su, "Neural control of bimanual robots with guaranteed global stability and motion precision," *IEEE Trans. Ind. Informat.*, vol. 13, no. 3, pp. 1162–1171, Jun. 2017.
[19] K. B. Ngo, R. Mahony, and Z.-P. Jiang, "Integrator backstepping using barrier functions for systems with multiple state constraints," in *Proc. 44th IEEE Conf. Decis. Control*, Dec. 2005, pp. 8306–8312.
[20] K. P. Tee, S. S. Ge, and E. H. Tay, "Barrier Lyapunov functions for the control of output-constrained nonlinear systems," *Automatica*, vol. 45, no. 4, pp. 918–927, Apr. 2009.
[21] K. P. Tee, B. Ren, and S. S. Ge, "Control of nonlinear systems with time-varying output constraints," *Automatica*, vol. 47, no. 11, pp. 2511–2516, Nov. 2011.
[22] W. He, H. Huang, and S. S. Ge, "Adaptive neural network control of a robotic manipulator with time-varying output constraints," *IEEE Trans. Cybern.*, vol. 47, no. 10, pp. 3136–3147, Oct. 2017.
[23] J.-X. Xu and X. Jin, "State-constrained iterative learning control for a class of MIMO systems," *IEEE Trans. Autom. Control*, vol. 58, no. 5, pp. 1322–1327, May 2013.
[24] Y.-J. Liu and S. Tong, "Barrier Lyapunov functions-based adaptive control for a class of nonlinear pure-feedback systems with full state constraints," *Automatica*, vol. 64, pp. 70–75, Feb. 2016.
[25] Y.-J. Liu and S. Tong, "Barrier Lyapunov functions for Nussbaum gain adaptive control of full state constrained nonlinear systems," *Automatica*, vol. 76, pp. 143–152, Feb. 2017.
[26] B. Xu, Z. Shi, F. Sun, and W. He, "Barrier lyapunov function based learning control of hypersonic flight vehicle with AOA constraint and actuator faults," *IEEE Trans. Cybern.*, to be published, doi: 10.1109/TCYB.2018.2794972.
[27] L. Ma and D. Li, "Adaptive neural networks control using barrier Lyapunov functions for dc motor system with time-varying state constraints," *Complexity*, vol. 2018, Jan. 2018, Art. no. 5082401, doi: 10.1155/2018/5082401.
[28] S. Wang, X. Ren, J. Na, and T. Zeng, "Extended-state-observer-based funnel control for nonlinear servomechanisms with prescribed tracking performance," *IEEE Trans. Autom. Sci. Eng.*, vol. 14, no. 1, pp. 98–108, Jan. 2017.
[29] Q. Chen, X. Tang, Y. Nan, and X. Ren, "Finite-time neural funnel control for motor servo systems with unknown input constraint," *J. Syst. Sci. Complex.*, vol. 30, no. 3, pp. 579–594, Jun. 2017.
[30] T. Berger, H. Le, and T. Reis, "Funnel control for nonlinear systems with known strict relative degree," *Automatica*, vol. 87, pp. 345–357, Jan. 2018.
[31] Q. Hu and X. Tan, "Unified attitude control for spacecraft under velocity and control constraints," *Aerosp. Sci. Technol.*, vol. 67, pp. 257–264, Aug. 2017.
[32] Q. Hu, "Robust adaptive backstepping attitude and vibration control with L_2-gain performance for flexible spacecraft under angular velocity constraint," *J. Sound Vib.*, vol. 327, no. 3, pp. 285–298, Nov. 2009.
[33] Q. Hu, B. Li, and Y. Zhang, "Robust attitude control design for spacecraft under assigned velocity and control constraints," *ISA Trans.*, vol. 52, no. 4, pp. 480–493, Jul. 2013.
[34] L. Sun, W. Huo, and Z. Jiao, "Adaptive backstepping control of spacecraft rendezvous and proximity operations with input saturation and full-state constraint," *IEEE Trans. Ind. Electron.*, vol. 64, no. 1, pp. 480–492, Jan. 2017.
[35] Q. Hu, X. Shao, and L. Guo, "Adaptive fault-tolerant attitude tracking control of spacecraft with prescribed performance," *IEEE/ASME Trans. Mech.*, vol. 23, no. 1, pp. 331–341, Feb. 2018.
[36] K. Lu and Y. Xia, "Finite-time attitude control for rigid spacecraft-based on adaptive super-twisting algorithm," *IET Control Theory Appl.*, vol. 8, no. 15, pp. 1465–1477, Oct. 2014.
[37] K. Lu and Y. Xia, "Adaptive attitude tracking control for rigid spacecraft with finite-time convergence," *Automatica*, vol. 49, no. 12, pp. 3591–3599, 2013.
[38] J. Han, "From PID to active disturbance rejection control," *IEEE Trans. Ind. Electron.*, vol. 56, no. 3, pp. 900–906, Mar. 2009.
[39] B.-Z. Guo and Z.-L. Zhao, "On convergence of tracking differentiator," *Int. J. Control*, vol. 84, no. 4, pp. 693–701, Apr. 2011.
[40] K. Lu, Y. Xia, Z. Zhu, and M. V. Basin, "Sliding mode attitude tracking of rigid spacecraft with disturbances," *J. Franklin Inst.*, vol. 349, no. 2, pp. 413–440, Mar. 2012.

ZHONGTIAN CHEN received the B.E. degree in chemical engineering and technology from the Beijing University of Chemical Technology, Beijing, China, in 2011.

He is currently pursuing the Ph.D. degree with the College of Information Engineering, Zhejiang University of Technology, Hangzhou, China. His research interests include spacecraft attitude control and fault-tolerant control.

QIANG CHEN received the B.S. degree in measurement and control technology and instrumentation from Hebei Agricultural University, Baoding, China, in 2006, and the Ph.D. degree in control science and engineering from the Beijing Institute of Technology, Beijing, China, in 2012.

He is currently an Associate Professor with the College of Information Engineering, Zhejiang University of Technology, Hangzhou, China. His research interests include neural networks, sliding-mode control, and adaptive control.

XIONGXIONG HE received the M.S. degree from Qufu Normal University, Qufu, China, in 1994, and the Ph.D. degree from Zhejiang University, Hangzhou, China, in 1997. He held a post-doctoral position with the Harbin Institute of Technology from 1998 to 2000.

In 2001, he joined the Zhejiang University of Technology, Hangzhou, where he is currently a Professor with the College of Information Engineering. His research areas include nonlinear control and signal processing.

MINGXUAN SUN received the B.E. degree in automatic control from the Xi'an University of Technology, Xi'an, China, in 1982, the M.E. degree in automatic control from the Beijing Institute of Technology, Beijing, China, in 1987, and the Ph.D. degree in electrical and electronic engineering from Nanyang Technological University, Singapore, in 2002.

In 1982, he joined the Hefei General Machinery Research Institute, Hefei, China, where he was an Assistant Engineer in 1983. From 1997 to 1998, he was the Deputy Director of the Department of Electronic Engineering, Xi'an Institute of Technology, Xi'an, where he has been an Associate Professor since 1994. He was a Research Fellow with Nanyang Technological University from 2001 to 2002 and with the National University of Singapore for one year. In 2004, he joined the College of Information Engineering, Zhejiang University of Technology, Hangzhou, China, where he has been a Professor since 2004. He teaches and conducts researches in the areas of iterative learning and repetitive control, nonlinear adaptive and robust control, neural networks and fuzzy systems, and control applications. He has co-authored one book and over 100 papers in journals and conference proceedings.